On estimating physical and chemical properties of hydrocarbon fuels using mid-infrared FTIR spectra and regularized linear models

Yu Wang[a,*], Yiming Ding[a], Wei Wei[a], Yi Cao, David F Davidson[a], Ronald K Hanson[a]

[a]*Stanford University, Stanford, California 94305*

Abstract

The concept of a compact, economical FTIR-based analyzer for estimating the properties of hydrocarbon fuels with small amounts of fuel is proposed. The high correlations between mid-IR FTIR absorption spectra of fuel vapor in the range 3300 to 3550 nm and 15 physical and chemical properties, such as density, initial boiling point, surface tension, kinematic viscosity, number of carbon and hydrogen per average molecule, and derived cetane number, for 64 hydrocarbon fuels are demonstrated. Lasso-regularized linear models based on linear combination of absorption cross sections at selected wavelengths are built for each of these physical and chemical properties, yielding accurate estimations.

Keywords: Hydrocarbon fuel, alternative fuel, physical and chemical property, combustion, mid-IR spectroscopy, generalized linear model, machine learning

*Corresponding author
Email address: yuwangme@stanford.edu (Yu Wang)

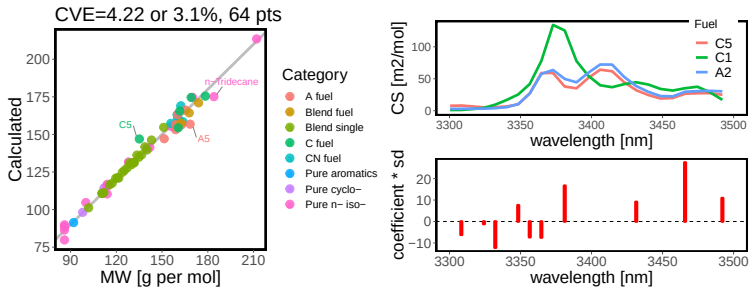

(a) (b)

Figure 9: Molecular weight [g/mol]. (a) Calculated MW using unnormalized spectrum. (b) Example spectra and selected λs and variation calculated at each λ.

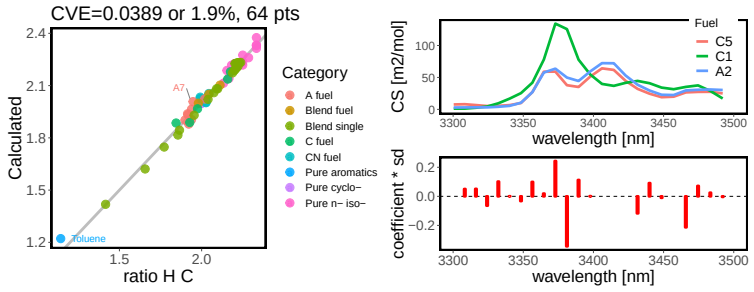

(a) (b)

Figure 10: Hydrogen to carbon ratio. (a) Calculated H/C ratio using unnormalized spectrum. (b) Example spectra and selected λs and variation calculated at each λ.

this property and this training dataset regardless of whether it is truly linear in mole fractions. The percentage cross validation error (column "%") in Table 2 is a measure of the approximation quality. For instance, denote two fuels with average molecular formula $C_{m_1}H_{n_1}$, $C_{m_2}H_{n_2}$ with hydrogen to carbon ratio (H/C ratio) $r_1 = \frac{n_1}{m_1}, r_2 = \frac{n_2}{m_2}$ and consider their mixture with mole fractions $x_1, x_2 = 1 - x_1$. Then the H/C ratio of the mixture, as derived in the equations below, is clearly not linear in mole fractions x_1, x_2, but interpolation $x_1 r_1 + x_2 r_2$ can be used as a reasonable approximation considering that the percentage cross validation error is 1.9% (Table 2). The quality of approximation can also be seen from Figure 10a.

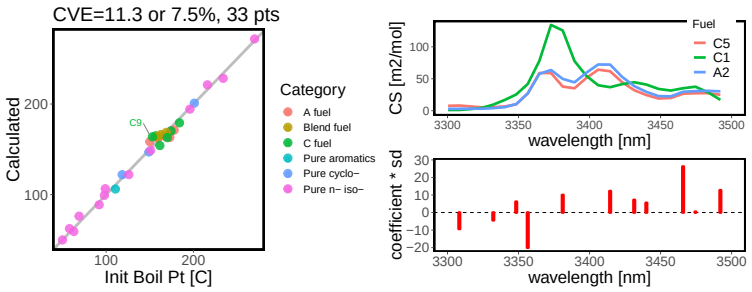

(a) (b)

Figure 11: Initial boiling point [°C] by ASTM D86. Data are taken from [43]. (a) Calculated IBP using unnormalized spectrum. (b) Example spectra and selected λs and variation calculated at each λ.

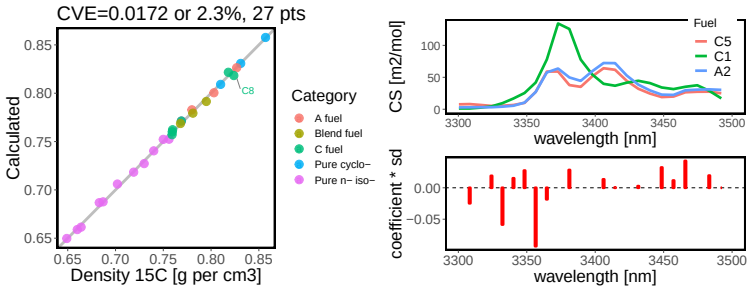

(a) (b)

Figure 12: Density [g/cm^3] at 15° C by ASTM D4052, or at 20°C. Data are taken from [43]. (a) Calculated density using normalized spectrum. (b) Example spectra and selected λs and variation calculated at each λ.

$$r_m = \frac{x_1 m_1 r_1 + x_2 m_2 r_2}{x_1 m_1 + x_2 m_2} \tag{8}$$

$$= \frac{x_1}{x_1 + x_2 \frac{m_2}{m_1}} r_1 + \frac{x_2}{x_1 \frac{m_1}{m_2} + x_2} r_2 \tag{9}$$

$$= \frac{x_1}{1 + x_2 (\frac{m_2}{m_1} - 1)} r_1 + \frac{x_2}{1 + x_1 (\frac{m_1}{m_2} - 1)} r_2 \tag{10}$$

Importantly, the regularized linear models proposed above can still estimate physical and chemical properties of hydrocarbon fuels based on its measured FTIR spectrum even if the property data for each component is not available.

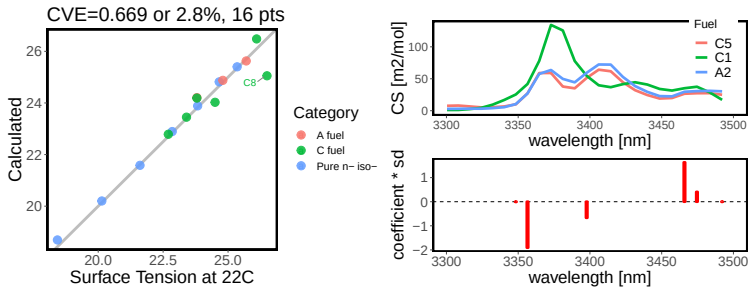

(a) (b)

Figure 13: Surface tension [dynes/cm] by ASTM D1331. (a) Calculated surface tension using unnormalized spectrum. (b) Example spectra and selected λs and variation calculated at each λ.

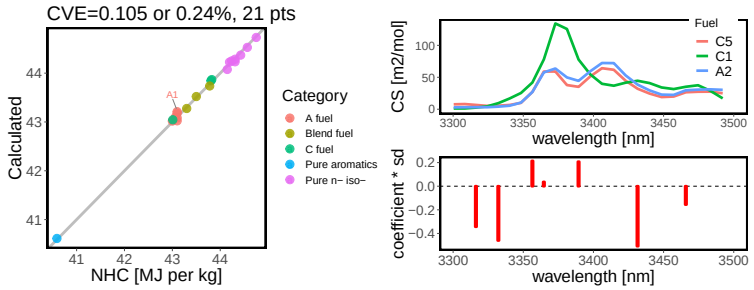

(a) (b)

Figure 14: Net heat of combustion [MJ/kg] by ASTM D4809. (a) Calculated NHC using normalized spectrum. (b) Example spectra and selected λs and variation calculated at each λ.

This is one of the advantages of using vapor phase spectra as described in more detail in subsection 2.1.

4.3. R language and RStudio

Training and cross validation of the regularized linear models are performed with the R language [53] using RStudio, specifically the `glmnet` package [54, 55] and `cv.glmnet` function, which were developed by researchers in the statistics department at Stanford University.

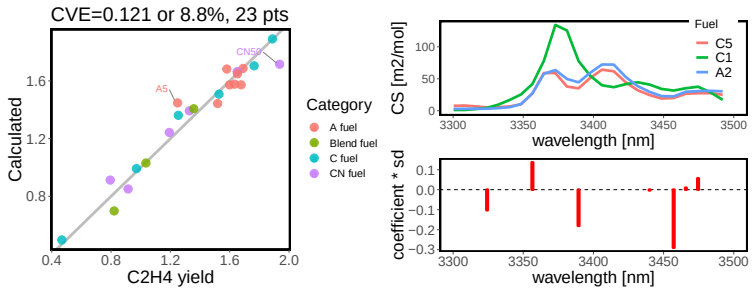

(a) (b)

Figure 15: C_2H_4 yield at 1300 K, 4 atm and 2 ms. It is defined as the mole fraction of C_2H_4 produced at 2 ms in a jet fuel pyrolysis experiment at 1300 K and 4 atm divided by the initial jet fuel mole fraction. Data are taken from [46]. (a) Calculated C_2H_4 yield using normalized spectrum. (b) Example spectra and selected λs and variation calculated at each λ.

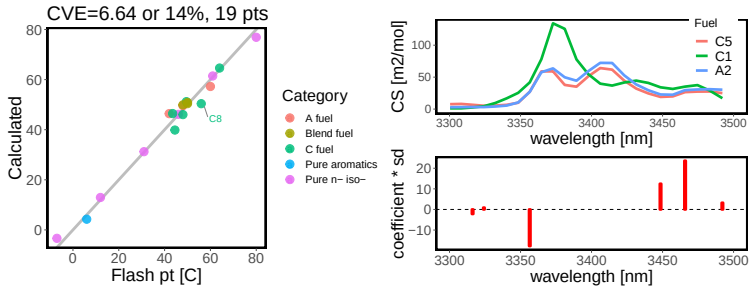

(a) (b)

Figure 16: Flash point [°C] by ASTM D93. Data are taken from [43]. (a) Calculated FP using unnormalized spectrum. (b) Example spectra and selected λs and variation calculated at each λ.

5. Conclusion

FTIR spectroscopy is used to provide the complete spectrum for unreacted hydrocarbon fuel vapor in the range 3300 to 3550 nm. Absorption cross sections in this wavelength region contain quantitative information about molecular structure. Different properties are most sensitive to different wavelengths, which in turn confirms the benefit of using the full spectrum. Spectral data can be combined with more sophisticated statistical models, such as the regularized

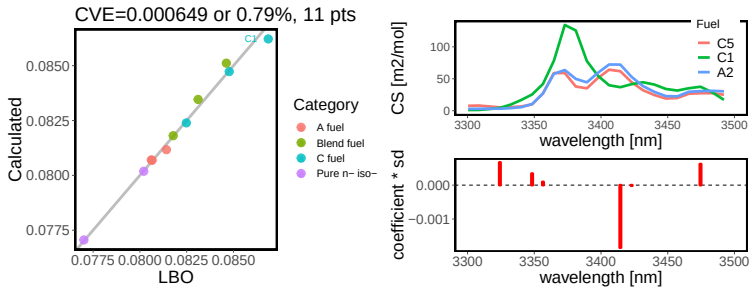

(a) (b)

Figure 17: LBO. (a) Calculated LBO using unnormalized spectrum. (b) Example spectra and selected λs and variation calculated at each λ.

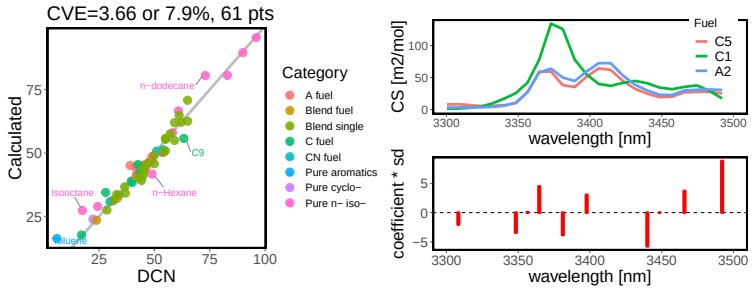

(a) (b)

Figure 18: DCN by ASTM D6890. Data are taken from [40, 41, 42]. (a) Calculated DCN using unnormalized spectrum. (b) Example spectra and selected λs and variation calculated at each λ.

linear model as demonstrated, to provide accurate estimations.

6. Acknowledgement

This work was funded in part by the U.S. Federal Aviation Administration (FAA) Office of Environment and Energy as a part of ASCENT Project 25 under FAA Award Number: 13-C-AJFE-SU-016. Any opinions, findings, and conclusions or recommendations expressed in this material are those of the authors and do not necessarily reflect the views of the FAA or other ASCENT sponsors.

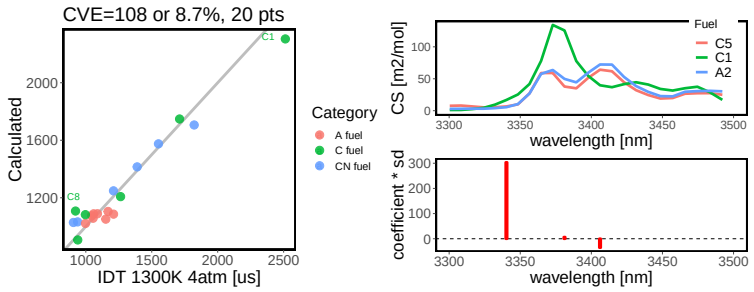

(a) (b)

Figure 19: IDT at 1300 K, 4 atm, with equivalence ratio 1. Data are taken from [46]. (a) Calculated IDT using unnormalized spectrum. (b) Example spectra and selected λs and variation calculated at each λ.

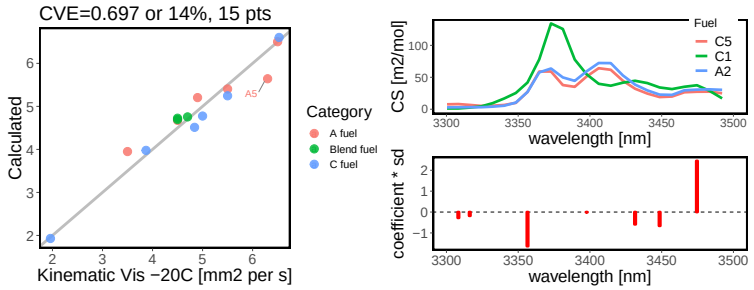

(a) (b)

Figure 20: Kinematic viscosity [mm/s] at -20°C by ASTM D445. (a) Calculated kinematic viscosity using unnormalized spectrum. (b) Example spectra and selected λs and variation calculated at each λ.

This work was also supported by the U.S. Air Force Office of Scientific Research through AFOSR Grant No. FA9550-16-1-0195, with Dr. Chiping Li as contract monitor. DISTRIBUTION A. Approved for public release: distribution unlimited.

Finally, much of the spectral data utilized were obtained in work supported by the U.S. Army Research Laboratory and the U.S. Army Research Office under contract/grant number W911-NF-17-1-0420.

The authors thank Dr. Christopher L. Strand for reviewing the paper.

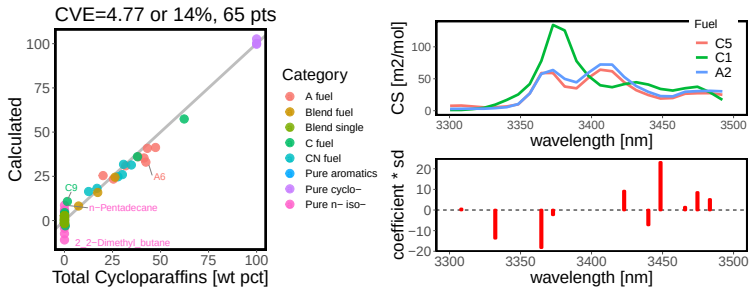

(a) (b)

Figure 21: Total cycloparaffin weight percentage. (a) Calculated total cycloparaffin weight percentage using normalized spectrum. (b) Example spectra and selected λs and variation calculated at each λ.

Declaration of interest

None.

References

[1] M. Colket, J. Heyne, M. Rumizen, M. Gupta, T. Edwards, W. M. Roquemore, G. Andac, R. Boehm, J. Lovett, R. Williams, J. Condevaux, D. Turner, N. Rizk, J. Tishkoff, C. Li, J. Moder, D. Friend, V. Sankaran, Overview of the National Jet Fuels Combustion Program, AIAA Journal 55 (2017) 1087–1104.

[2] J. S. Heyne, M. B. Colket, M. Gupta, A. Jardines, J. P. Moder, J. T. Edwards, M. Roquemore, C. Li, M. Rumizen, Year 2 of the National Jet Fuels Combustion Program: Towards a Streamlined Alternative Jet Fuels Certification Process, 55th AIAA Aerospace Sciences Meeting (2017) 1–14.

[3] J. S. Heyne, E. Peiffer, M. B. Colket, A. Jardines, C. Shaw, J. P. Moder, W. M. Roquemore, J. T. Edwards, C. Li, M. Rumizen, M. Gupta, Year 3 of the National Jet Fuels Combustion Program: Practical and Scientific Impacts of Alternative Jet Fuel Research, in: 2018 AIAA Aerospace Sci-

ences Meeting, volume 812, 2018. URL: https://arc.aiaa.org/doi/10.2514/6.2018-1667. doi:10.2514/6.2018-1667.

[4] Allied Market Research, Global Opportunity Analysis and Industry Forecast, 2014 - 2022, 2016. URL: https://www.alliedmarketresearch.com/alternative-fuel-and-hybrid-vehicle-market.

[5] T. Parise, D. F. Davidson, R. K. Hanson, Shock tube/laser absorption measurements of the pyrolysis of a bimodal test fuel, Proceedings of the Combustion Institute 36 (2017) 281–288.

[6] J. Shao, R. Choudhary, Y. Peng, D. F. Davidson, R. K. Hanson, A shock tube study of n-heptane, iso-octane, n-dodecane and iso-octane/n-dodecane blends oxidation at elevated pressures and intermediate temperatures, Fuel 243 (2019) 541–553.

[7] A. M. Ferris, D. F. Davidson, R. K. Hanson, A combined laser absorption and gas chromatography sampling diagnostic for speciation in a shock tube, Combustion and Flame 195 (2018) 40–49.

[8] S. Wang, R. K. Hanson, Ultra-sensitive spectroscopy of OH radical in high-temperature transient reactions, Optics Letters 43 (2018) 3518.

[9] W. Wei, W. Y. Peng, Y. Wang, R. Choudhary, S. Wang, J. Shao, R. K. Hanson, Demonstration of non-absorbing interference rejection using wavelength modulation spectroscopy in high-pressure shock tubes, Applied Physics B: Lasers and Optics 125 (2019) 9.

[10] S. Wang, D. F. Davidson, R. K. Hanson, Shock tube measurements of OH concentration time-histories in benzene, toluene, ethylbenzene and xylene oxidation, Proceedings of the Combustion Institute 37 (2019) 163–170.

[11] W. Y. Peng, Y. Wang, J. Cassady, C. L. Strand, R. K. Hanson, Single-Ended Sensor for Thermometry and Speciation in Shock Tubes Using Native Surfaces, IEEE Sensors XX (2019) 1–8.

[12] J. T. Edwards, Reference Jet Fuels for Combustion Testing, 55th AIAA Aerospace Sciences Meeting (2017) 1–58.

[13] H. Wang, R. Xu, K. Wang, C. T. Bowman, R. K. Hanson, D. F. Davidson, K. Brezinsky, F. N. Egolfopoulos, A physics-based approach to modeling real-fuel combustion chemistry - I. Evidence from experiments, and thermodynamic, chemical kinetic and statistical considerations, Combustion and Flame 193 (2018) 502–519.

[14] R. Xu, K. Wang, S. Banerjee, J. Shao, T. Parise, Y. Zhu, S. Wang, A. Movaghar, D. J. Lee, R. Zhao, X. Han, Y. Gao, T. Lu, K. Brezinsky, F. N. Egolfopoulos, D. F. Davidson, R. K. Hanson, C. T. Bowman, H. Wang, A physics-based approach to modeling real-fuel combustion chemistry – II. Reaction kinetic models of jet and rocket fuels, Combustion and Flame 193 (2018) 520–537.

[15] Y. Tao, R. Xu, K. Wang, J. Shao, S. E. Johnson, A. Movaghar, X. Han, J.-W. Park, T. Lu, K. Brezinsky, F. N. Egolfopoulos, D. F. Davidson, R. K. Hanson, C. T. Bowman, H. Wang, A Physics-based approach to modeling real-fuel combustion chemistry – III. Reaction kinetic model of JP10, Combustion and Flame 198 (2018) 466–476.

[16] K. Wang, R. Xu, T. Parise, J. Shao, A. Movaghar, D. J. Lee, J.-W. Park, Y. Gao, T. Lu, F. N. Egolfopoulos, D. F. Davidson, R. K. Hanson, C. T. Bowman, H. Wang, A physics-based approach to modeling real-fuel combustion chemistry – IV. HyChem modeling of combustion kinetics of a bio-derived jet fuel and its blends with a conventional Jet A, Combustion and Flame 198 (2018) 477–489.

[17] N. Zanier-Szydlowski, A. Quignard, F. Baco, H. Biguerd, L. Carpot, F. Wahl, Control of Refining Processes on Mid-Distillates by Near Infrared Spectroscopy, Oil and Gas Science and Technology 54 (1999) 463–472.

[18] R. M. Balabin, E. I. Lomakina, Support vector machine regression

(SVR/LS-SVM) - An alternative to neural networks (ANN) for analytical chemistry? Comparison of nonlinear methods on near infrared (NIR) spectroscopy data, Analyst 136 (2011) 1703–1712.

[19] A. R. Torres, G. M. Xavier, M. L. Paredes, C. L. Cunha, A. S. Luna, R. C. Oliveira, Predicting the properties of biodiesel and its blends using mid-FT-IR spectroscopy and first-order multivariate calibration, Fuel 204 (2017) 185–194.

[20] J. C. L. Alves, C. B. Henriques, R. J. Poppi, Determination of diesel quality parameters using support vector regression and near infrared spectroscopy for an in-line blending optimizer system, Fuel 97 (2012) 710–717.

[21] M. P. F. Da Silva, L. R. E. Brito, F. A. Honorato, A. P. S. Paim, C. Pasquini, M. F. Pimentel, Classification of gasoline as with or without dispersant and detergent additives using infrared spectroscopy and multivariate classification, Fuel 116 (2014) 151–157.

[22] P. A. Pantoja, J. López-Gejo, C. A. O. do Nascimento, G. A. C. L. Roux, Application of Near-Infrared Spectroscopy to the Characterization of Petroleum, Technical Report, 2017. URL: https://onlinelibrary.wiley.com/doi/pdf/10.1002/9781119286325.ch8. doi:10.1002/9781119286325.ch8.

[23] C. Pasquini, A. F. Bueno, Characterization of petroleum using near-infrared spectroscopy: Quantitative modeling for the true boiling point curve and specific gravity, Fuel 86 (2007) 1927–1934.

[24] U. Hoffmann, N. Zanier-Szydlowski, Portability of near infrared spectroscopic calibrations for petrochemical parameters, Journal of Near Infrared Spectroscopy 7 (1999) 33–45.

[25] Z.-N. Xing, J.-X. Wang, Y. Ye, G. Shen, Rapid Quantification of Kinematical Viscosity in Aviation Kerosene by Near-Infrared Spectroscopy (2006).

[26] P. Felizardo, P. Baptista, M. S. Uva, J. C. Menezes, M. J. Neiva Correia, Monitoring biodiesel fuel quality by near infrared spectroscopy, Journal of Near Infrared Spectroscopy 15 (2007) 97–105.

[27] D. J. Cookson, B. E. Smith, Calculation of Jet and Diesel Fuel Properties Using 13C NMR Spectroscopy, Energy and Fuels 4 (1990) 152–156.

[28] T. H. DeFries, R. V. Kastrup, D. Indritz, Prediction of cetane number by group additivity and carbon-13 Nuclear Magnetic Resonance, Industrial & Engineering Chemistry Research 26 (1987) 188–193.

[29] W. F. d. C. Rocha, D. A. Sheen, Determination of physicochemical properties of petroleum derivatives and biodiesel using GC/MS and chemometric methods with uncertainty estimation, Fuel 243 (2019) 413–422.

[30] P. Vozka, B. A. Modereger, A. C. Park, W. T. J. Zhang, R. W. Trice, H. I. Kenttämaa, G. Kilaz, Jet fuel density via GC x GC-FID, Fuel 235 (2019) 1052–1060.

[31] B. Creton, C. Dartiguelongue, T. De Bruin, H. H. Toulhoat, Prediction of the Cetane Number of Diesel Compounds Using the Quantitative Structure Property Relationship, Energy & Fuels 24 (2010) 5396–5403.

[32] D. A. Saldana, L. Starck, P. Mougin, B. Rousseau, L. Pidol, N. Jeuland, B. Creton, Flash point and cetane number predictions for fuel compounds using quantitative structure property relationship (QSPR) methods, Energy and Fuels 25 (2011) 3900–3908.

[33] D. A. Saldana, L. Starck, P. Mougin, B. Rousseau, B. Creton, On the rational formulation of alternative fuels: Melting point and net heat of combustion predictions for fuel compounds using machine learning methods, SAR and QSAR in Environmental Research 24 (2013) 525–543.

[34] D. A. Saldana, L. Starck, P. Mougin, B. Rousseau, N. Ferrando, B. Creton, Prediction of density and viscosity of biofuel compounds using machine learning methods, Energy and Fuels 26 (2012) 2416–2426.

[35] F. L. Dryer, Chemical kinetic and combustion characteristics of transportation fuels, Proceedings of the Combustion Institute 35 (2015) 117–144.

[36] S. W. Sharpe, T. J. Johnson, R. L. Sams, P. M. Chu, G. C. Rhoderick, P. A. Johnson, Gas-phase databases for quantitative infrared spectroscopy, Applied Spectroscopy 58 (2004) 1452–1461.

[37] Y. Wang, Y. Cao, D. F. Davidson, R. K. Hanson, Ignition delay time measurements for distillate and synthetic jet fuels, in: AIAA Scitech 2019 Forum, American Institute of Aeronautics and Astronautics, Reston, Virginia, 2019. URL: http://arc.aiaa.orghttps://arc.aiaa.org/doi/10.2514/6.2019-2248. doi:10.2514/6.2019-2248.

[38] R. Q. Casselberry, E. Corporan, M. J. DeWitt, Correlation of combustor lean blowout performance to supercritical pyrolysis products, Fuel 252 (2019) 504–511.

[39] E. Corporan, J. T. Edwards, S. Stouffer, M. DeWitt, Z. West, C. Klingshirn, C. Bruening, Impacts of Fuel Properties on Combustor Performance, Operability and Emissions Characteristics, in: 55th AIAA Aerospace Sciences Meeting, American Institute of Aeronautics and Astronautics, Reston, Virginia, 2017. URL: http://arc.aiaa.org/doi/10.2514/6.2017-0380. doi:10.2514/6.2017-0380.

[40] M. J. Murphy, J. D. Taylor, R. L. McCormick, Compendium of Experimental Cetane Number Data, Technical Report, 2004. URL: http://www.osti.gov/servlets/purl/1086353/. doi:10.2172/1086353.

[41] S. Dooley, S. H. Won, M. Chaos, J. Heyne, Y. Ju, F. L. Dryer, K. Kumar, C. J. Sung, H. Wang, M. A. Oehlschlaeger, R. J. Santoro, T. A. Litzinger, A jet fuel surrogate formulated by real fuel properties, Combustion and Flame 157 (2010) 2333–2339.

[42] S. H. Won, S. Dooley, P. S. Veloo, H. Wang, M. A. Oehlschlaeger, F. L. Dryer, Y. Ju, The combustion properties of 2,6,10-trimethyl dodecane and

a chemical functional group analysis, Combustion and Flame 161 (2014) 826–834.

[43] Engineering ToolBox, Hydrocarbons - physical data, 2017. URL: https://www.engineeringtoolbox.com/hydrocarbon-boiling-melting-flash-autoignition-point-density-gravity-molweight-d{_}1966.html.

[44] B. Smith, Fundamentals of Fourier Transform Infrared Spectroscopy, Second Edition, CRC Press, 2011. URL: https://www.taylorfrancis.com/books/9781420069303. doi:10.1201/b10777. arXiv:arXiv:1011.1669v3.

[45] A. E. Klingbeil, J. B. Jeffries, R. K. Hanson, Temperature-dependent mid-IR absorption spectra of gaseous hydrocarbons, Journal of Quantitative Spectroscopy and Radiative Transfer 107 (2007) 407–420.

[46] Y. Wang, Y. Cao, W. Wei, D. F. Davidson, R. K. Hanson, A new method of estimating derived cetane number for hydrocarbon fuels, Fuel 241 (2019) 319–326.

[47] J. J. Workman, Interpretive spectroscopy for near infrared, Applied Spectroscopy Reviews 31 (1996) 251–320.

[48] G. Socrates, Infrared and Raman characteristic group frequencies, John Wiley & Sons, 2004. doi:10.1002/jrs.1238. arXiv:arXiv:1011.1669v3.

[49] Q. Wang, Y. Hou, W. Wu, M. Niu, S. Ren, Z. Liu, The relationship between the humic degree of oil shale kerogens and their structural characteristics, Fuel 209 (2017) 35–42.

[50] M. R. Riazi, Characterization Petroleum and Properties of Fractions, 2005. URL: http://www.copyright.com/.https://www.cambridge.org/core/product/identifier/CBO9781107415324A009/type/book{_}part.

[51] R. Kohavi, A study of cross-validation and bootstrap for accuracy estimation and model selection, Proceedings of the 14th international joint conference on Artificial intelligence - Volume 2 2 (1995) 1137–1143.

[52] T. Hastie, R. Tibshirani, J. Friedman, Springer Series in The Elements of Statistical Learning, 2009. doi:10.1007/978-0-387-98135-2. arXiv:arXiv:1011.1669v3.

[53] R Core Team, R: A Language and Environment for Statistical Computing, R Foundation for Statistical Computing, Vienna, Austria, 2019. URL: https://www.R-project.org.

[54] J. Friedman, T. Hastie, R. Tibshirani, Regularization Paths for Generalized Linear Models via Coordinate Descent, Journal of Statistical Software 33 (2015).

[55] N. Simon, J. Friedman, T. Hastie, R. Tibshirani, Regularization Paths for Cox's Proportional Hazards Model via Coordinate Descent, Journal of Statistical Software 39 (2015).

Table 3: Wavelengths [nm] and coefficients for average number of carbon atoms. Intercept $\beta_0^* = -1.64$.

	w1	w2	w3	w4	w5	w6	w7	w8	w9	w10	w11
λ^*	3300.4	3308.3	3324.2	3332.2	3348.4	3356.5	3364.7	3381.1	3431.5	3465.9	3492.1
β^*	9.6E-01	-3.2E-01	-5.3E-02	-5.9E-01	1.2E-01	-6.3E-02	-3.5E-02	5.5E-02	5.9E-02	3.2E-01	4.8E-02

Table 4: Wavelengths [nm] and coefficients for average number of hydrogen atoms. Intercept $\beta_0^* = -2.91$.

	w1	w2	w3	w4	w5	w6	w7	w8	w9	w10	w11
λ^*	3300.4	3308.3	3324.2	3332.2	3348.4	3381.1	3414.5	3431.5	3465.9	3474.6	3492.1
β^*	1.3E+00	-5.3E-01	-5.5E-01	-3.3E-01	7.3E-02	8.4E-02	1.1E-02	1.3E-01	3.7E-01	1.7E-02	1.1E-01

Table 5: Wavelengths [nm] and coefficients for MW [g/mol]. Intercept $\beta_0^* = -22.7$.

	w1	w2	w3	w4	w5	w6	w7	w8	w9	w10	w11
λ^*	3300.4	3308.3	3324.2	3332.2	3348.4	3356.5	3364.7	3381.1	3431.5	3465.9	3492.1
β^*	1.3E+01	-4.4E+00	-1.3E+00	-7.4E+00	1.5E+00	-7.6E-01	-4.2E-01	7.4E-01	8.5E-01	4.2E+00	6.9E-01

Table 6: Wavelengths [nm] and coefficients for ratio H/C. Intercept $\beta_0^* = 2.14$.

	w1	w2	w3	w4	w5	w6	w7	w8	w9	w10	w11	w12	w13	w14	w15	w16	w17	w18	w19	w20
λ^*	3300.4	3308.3	3316.2	3324.2	3332.2	3340.3	3348.4	3356.5	3364.7	3372.9	3381.1	3389.4	3397.7	3431.5	3440.0	3448.6	3465.9	3474.6	3483.3	3492.1
β^*	-1.1E-01	3.6E-02	5.4E-02	-7.1E-02	6.1E-02	2.5E-04	-6.6E-03	1.0E-02	1.1E-03	9.7E-03	-1.5E-02	9.4E-03	8.2E-05	-1.1E-02	9.7E-03	-1.6E-03	-3.2E-02	1.1E-02	2.5E-03	-2.6E-04

Table 7: Wavelengths [nm] and coefficients for initial boiling point [°C]. Intercept $\beta_0^* = -20.0$.

	w1	w2	w3	w4	w5	w6	w7	w8	w9	w10	w11	w12
λ^*	3300.4	3308.3	3332.2	3348.4	3356.5	3381.1	3414.5	3431.5	3440.0	3465.9	3474.6	3492.1
β^*	1.3E+01	-5.7E+00	-2.0E+00	1.0E+00	-1.7E+00	3.9E-01	2.8E-01	5.9E-01	5.0E-01	3.6E+00	6.8E-02	6.4E-01

Table 8: Wavelengths [nm] and coefficients for density at 15°C [g/cm^3]. Intercept $\beta_0^* = 0.314$.

	w1	w2	w3	w4	w5	w6	w7	w8	w9	w10	w11	w12	w13	w14	w15	w16	w17
λ^*	3300.4	3308.3	3324.2	3332.2	3340.3	3348.4	3356.5	3364.7	3381.1	3406.1	3414.5	3431.5	3448.6	3457.2	3465.9	3483.3	3492.1
β^*	1.4E+02	-1.0E+02	1.2E+02	-2.1E+02	3.1E+01	2.4E+01	-3.9E+01	-5.9E+00	8.7E+00	3.5E+00	6.0E-02	2.2E+00	4.5E+01	1.6E+01	5.9E+01	2.6E+01	-2.7E-03

Table 9: Wavelengths [nm] and coefficients for Surface Tension at 22°C [dynes/cm]. Intercept $\beta_0^* = 19.7$.

	w1	w2	w3	w4	w5	w6	w7
w	3300.4	3348.4	3356.5	3397.7	3465.9	3474.6	3492.1
c	1.3E-01	-1.6E-03	-3.0E-01	-4.6E-02	4.1E-01	1.2E-01	-2.9E-04

Table 10: Wavelengths [nm] and coefficients for NHC [MJ/kg]. Intercept $\beta_0^* = 48.5$.

	w1	w2	w3	w4	w5	w6	w7
λ^*	3316.2	3332.2	3356.5	3364.7	3389.4	3431.5	3465.9
β^*	-2.9E+02	-6.2E+02	1.9E+02	2.0E+01	1.8E+02	-8.9E+02	-4.6E+02

Table 11: Wavelengths [nm] and coefficients for C2H4 yield. Intercept $\beta_0^* = 5.05$.

	w1	w2	w3	w4	w5	w6	w7	w8
λ^*	3300.4	3324.2	3356.5	3389.4	3440.0	3457.2	3465.9	3474.6
β^*	9.3E+01	-9.8E+02	2.6E+02	-2.0E+02	-1.5E+01	-1.7E+03	7.1E+01	5.8E+02

Table 12: Wavelengths [nm] and coefficients for flash point [°C]. Intercept $\beta_0^* = -51.9$.

	w1	w2	w3	w4	w5	w6	w7
λ^*	3300.4	3316.2	3324.2	3356.5	3448.6	3465.9	3492.1
β^*	4.1E+00	-2.0E+00	1.1E+00	-2.0E+00	1.7E+00	3.4E+00	2.1E-01

Table 13: Wavelengths [nm] and coefficients for LBO. Intercept $\beta_0^* = 0.0762$.

	w1	w2	w3	w4	w5	w6
λ^*	3324.2	3348.4	3356.5	3414.5	3423.0	3474.6
β^*	7.9E-04	5.8E-05	1.3E-05	-6.1E-05	-1.8E-06	1.8E-04

Table 14: Wavelengths [nm] and coefficients for DCN. Intercept $\beta_0^* = 26.7$.

	w1	w2	w3	w4	w5	w6	w7	w8	w9	w10	w11
λ^*	3300.4	3308.3	3348.4	3356.5	3364.7	3381.1	3397.7	3440.0	3448.6	3465.9	3492.1
β^*	-6.9E-02	-1.4E+00	-7.6E-01	9.2E-03	2.8E-01	-1.7E-01	1.7E-01	-6.9E-01	-2.0E-03	5.8E-01	5.6E-01

Table 15: Wavelengths [nm] and coefficients for IDT at 1300K, 4atm [μs]. Intercept $\beta_0^* = 748$.

	w1	w2	w3
λ^*	3340.3	3381.1	3406.1
β^*	9.8E+01	3.0E-01	-3.1E+00

Table 16: Wavelengths [nm] and coefficients for kinematic viscosity at -20°C [mm^2/s]. Intercept $\beta_0^* = -5.21$.

	w1	w2	w3	w4	w5	w6	w7	w8
λ^*	3300.4	3308.3	3316.2	3356.5	3397.7	3431.5	3448.6	3474.6
β^*	3.0E-03	-1.7E-01	-1.6E-01	-2.5E-01	-3.7E-03	-1.5E-01	-1.6E-01	8.9E-01

Table 17: Wavelengths [nm] and coefficients for Total Cycloparaffins [wt %]. Intercept $\beta_0^* = -138$.

	w1	w2	w3	w4	w5	w6	w7	w8	w9	w10	w11
λ^*	3300.4	3308.3	3332.2	3364.7	3372.9	3423.0	3440.0	3448.6	3465.9	3474.6	3483.3
β^*	1.1E+03	4.6E+02	-2.9E+04	-7.6E+03	-7.2E+02	5.0E+03	-8.1E+03	3.9E+04	2.4E+03	1.7E+04	8.1E+03

Table 18: List of fuels and their GC×GC compositions. The labeling of fuels is consistent with [46].

Category	Fuel	POSF	C	H	Total Aromatics [wt %]	Total Cycloparaffins [wt %]	Total iso Paraffins [wt %]	Total n Paraffins [wt %]
A fuel	A1	10264	10.8	21.8	13.4	20.1	39.7	26.8
A fuel	A2	10325	11.4	22.1	18.7	31.9	29.5	20.0
A fuel	A3	10289	11.9	22.6	20.6	47.4	18.1	13.9
A fuel	A4	12784	11.5	22.1	18.6	43.2	23.2	15.1
A fuel	A5	12831	12.1	23.2	18.2	41.4	25.2	15.2
A fuel	A6	12843	11.7	22.4	18.6	42.4	23.8	15.3
A fuel	A7	12905	11.5	22.4	21.2	25.5	29.6	23.8
A fuel	A8	12906	11.4	22.1	17.4	38.4	25.1	19.0
Blend fuel	20%A2-80%C1		12.3	26.0	4.3	7.3	83.6	4.6
Blend fuel	50%A2-50%C1		11.9	24.4	10.1	17.3	61.6	10.9
Blend fuel	80%A2-20%C1		11.6	23.0	15.4	26.3	41.7	16.5
Blend single	BF1		9.4	19.1	20.4	0.0	0.0	79.6
Blend single	BF10		8.4	16.4	47.9	0.0	26.0	26.1
Blend single	BF11		8.2	17.2	0.0	0.0	100.0	0.0
Blend single	BF12		8.0	14.9	29.8	0.0	35.4	34.9
Blend single	BF13		9.2	19.3	15.0	0.0	67.8	17.2
Blend single	BF14		8.6	17.8	38.4	0.0	43.9	17.7
Blend single	BF2		8.8	16.3	40.8	0.0	0.0	59.2
Blend single	BF3		7.6	10.7	80.4	0.0	0.0	19.6
Blend single	BF4		8.2	13.6	60.2	0.0	0.0	39.8
Blend single	BF5		9.6	21.2	100.0	0.0	0.0	0.0
Blend single	BF6		9.2	20.4	0.0	0.0	19.3	80.7
Blend single	BF7		8.8	19.6	0.0	0.0	39.7	60.3
Blend single	BF8		8.4	18.8	0.0	0.0	60.0	40.0
Blend single	BF9		8.0	14.3	0.0	0.0	79.9	20.1
Blend single	Won10		10.6	23.3	0.0	0.0	33.8	66.2
Blend single	Won11		8.7	19.4	0.0	0.0	64.6	35.4
Blend single	Won12		8.9	19.9	0.0	0.0	53.3	46.7
Blend single	Won13		9.2	20.4	0.0	0.0	39.0	61.0
Blend single	Won14		9.5	21.0	0.0	0.0	25.6	74.4
Blend single	Won15		9.9	21.7	0.0	0.0	6.6	93.4
Blend single	Won6		9.0	20.1	0.0	0.0	73.9	26.1
Blend single	Won7		9.4	20.8	0.0	0.0	65.4	34.7
Blend single	Won8		9.8	21.5	0.0	0.0	55.8	44.2
Blend single	Won9		10.1	22.2	0.0	0.0	48.1	51.9
		11498						
C fuel	C1	12368	12.6	27.2	0.0	0.1	99.6	0.0
		12384						
		12344						
C fuel	C4	12489	11.4	24.8	0.4	0.4	98.5	0.2
		12345						
		12713						
C fuel	C5	12789	9.7	18.7	30.7	0.1	51.6	17.7
		12816						
C fuel	C7	12925	12.1	23.9	4.9	62.3	29.5	3.3
C fuel	C8	12923	11.6	21.4	27.3	38.0	21.0	13.7
CN fuel	CN30	13197	11.6	23.1	13.1	12.6	65.0	9.4
CN fuel	CN35	13198	11.4	23.3	10.3	16.9	61.7	11.1
CN fuel	CN40	13199	11.7	23.3	12.8	27.8	47.8	11.6
CN fuel	CN45	13200	11.4	23.1	8.7	30.1	47.0	14.2
CN fuel	CN50	13201	11.1	22.5	8.3	34.8	39.4	17.5
CN fuel	CN55	13202	11.5	23.3	7.4	30.7	34.7	24.4
Pure aromatics	Toluene		7.0	8.0	100.0	0.0	0.0	0.0
Pure cyclo-	Cyclodecane		10.0	20.0	0.0	100.0	0.0	0.0
Pure cyclo-	Cycloheptane		7.0	14.0	0.0	100.0	0.0	0.0
Pure cyclo-	Cyclooctane		8.0	16.0	0.0	100.0	0.0	0.0
Pure n- iso-	2,2-Dimethyl_butane		6.0	14.0	0.0	0.0	100.0	0.0
Pure n- iso-	2,3-Dimethylbutane		6.0	14.0	0.0	0.0	100.0	0.0
Pure n- iso-	3-Methylhexane		8.0	18.0	0.0	0.0	100.0	0.0
Pure n- iso-	3-Methylpentane		6.0	14.0	0.0	0.0	100.0	0.0
Pure n- iso-	Isooctane		8.0	18.0	0.0	0.0	100.0	0.0
Pure n- iso-	n-Decane		10.0	22.0	0.0	0.0	0.0	100.0
Pure n- iso-	n-Dodecane		12.0	26.0	0.0	0.0	0.0	100.0
Pure n- iso-	n-Heptane		7.0	16.0	0.0	0.0	0.0	100.0
Pure n- iso-	n-Hexane		6.0	14.0	0.0	0.0	0.0	100.0
Pure n- iso-	n-Nonane		9.0	20.0	0.0	0.0	0.0	100.0
Pure n- iso-	n-Pentadecane		15.0	32.0	0.0	0.0	0.0	100.0
Pure n- iso-	n-Tridecane		13.0	28.0	0.0	0.0	0.0	100.0
Pure n- iso-	n-Undecane		11.0	24.0	0.0	0.0	0.0	100.0
Pure n- iso-	n-Octane		8.0	18.0	0.0	0.0	0.0	100.0

Table 19: Physical and chemical properties of fuels in the training dataset. The labeling of fuels is consistent with [46].

Category	Fuel	MW	ratio H/C	IBP [43]	Density [43]	ST	NHC	C2H4 yield [46]	FP	LBO [38, 39]	DCN [40, 41, 42]	IDT [46]	KV	Total cyclo
A fuel	A1	151.4	2.019	150	0.7799	23.8	43.1	1.58	42	0.08066	48.61	997.8	3.5	20.08
A fuel	A2	158.9	1.939	159.2	0.803	24.8	43.06	1.69	48	0.08061	48	1044	4.5	31.86
A fuel	A3	165.4	1.899	177.9	0.8268	25.7	43	1.599	60	0.08142	39.07	1059	6.5	47.39
A fuel	A4	160.1	1.922	168			43.1	1.518			41.52	1210	4.9	43.16
A fuel	A5	168.4	1.917	161			43.1	1.248			45.05	1151	6.3	41.4
A fuel	A6	162.8	1.915	173			43.1	1.633			41.91	1088	5.5	42.38
A fuel	A7	160.4	1.948					1.652			49.11	1169		25.48
A fuel	A8	158.9	1.939					1.677			46.34	1055		38.44
Blend fuel	20%A2-80%C1	173.9	2.112	168.8	0.768		43.78	0.821	50	0.08462	23.86		4.7	7.325
Blend fuel	50%A2-50%C1	167.8	2.045	162.5	0.781		43.5	1.035	50	0.08311	33.28		4.5	17.31
Blend fuel	80%A2-20%C1	162.3	1.98	158.3	0.795		43.3	1.358	48	0.08178	41.78		4.5	26.32
Blend single	BF1	131.8	2.039								62.14			0
Blend single	BF10	117.3	1.955								43.27			0
Blend single	BF11	115.5	2.098								32.99			0
Blend single	BF12	110.5	1.865								31.66			0
Blend single	BF13	129.9	2.091								57.14			0
Blend single	BF14	120.8	2.075								45.52			0
Blend single	BF2	121.6	1.856								54.14			0
Blend single	BF3	101.8	1.416								28.58			0
Blend single	BF4	111.9	1.656								44.18			0
Blend single	BF5	136.6	2.208								61.21			0
Blend single	BF6	130.9	2.217								55.08			0
Blend single	BF7	125.2	2.227								46.93			0
Blend single	BF8	119.6	2.238								36.59			0
Blend single	BF9	110.8	1.772								36.93			0
Blend single	Won10	151.1	2.188								65			0
Blend single	Won11	123.9	2.23								45			0
Blend single	Won12	127.1	2.224								50			0
Blend single	Won13	131.1	2.217								55			0
Blend single	Won14	134.8	2.211								59.1			0
Blend single	Won15	140.2	2.203								65			0
Blend single	Won6	128.6	2.221								45			0
Blend single	Won7	133.5	2.213								50			0
Blend single	Won8	138.8	2.205								55			0
Blend single	Won9	143.1	2.198								59.1			0
C fuel	C1	178.4	2.159	174.3	0.7597	23.4	43.82	0.468	49.5	0.08686	17.1	2513	5	0.05
C fuel	C4	161.6	2.175	161.5	0.7592	22.7	43.81	0.971	44.5	0.08477	28	1711	3.87	0.43
C fuel	C5	135.1	1.928	156.6	0.7689	23.8	43.01	1.764	43.5	0.08248	39.6	1264	1.96	0.07
C fuel	C7	169.1	1.975	184	0.8181	26.1		1.528	64		42.6	939	6.53	62.31
C fuel	C8	160.6	1.845	170	0.8238	26.5		1.254	56		43.5	922	4.84	37.97
CN fuel	CN30	162.3	1.991					0.915			30	1822		12.55
CN fuel	CN35	160.1	2.044					0.7946			34	1551		16.93
CN fuel	CN40	163.7	1.991					1.193			40	1390		27.83
CN fuel	CN45	159.9	2.026					1.328			44	1210		30.14
CN fuel	CN50	155.7	2.027					1.937			51	937.8		34.81
CN fuel	CN55	161.3	2.026					1.65			54	906		30.74
Pure aromatics	Toluene	92	1.143	110.6			40.59		6		6			0
Pure cyclo-	Cyclodecane	140	2	201	0.857									100
Pure cyclo-	Cycloheptane	98	2	118.4	0.81									100
Pure cyclo-	Cyclooctane	112	2	149	0.831						22.3			100
Pure n- iso-	2,2-Dimethylbutane	86	2.333	50	0.649						24.4			0
Pure n- iso-	2,3-Dimethylbutane	86	2.333	58										0
Pure n- iso-	3-Methylhexane	114	2.25	92	0.687						42			0
Pure n- iso-	3-Methylpentane	86	2.333	63	0.66						30.7			0
Pure n- iso-	Isooctane	114	2.25	99			44.31				17.5			0
Pure n- iso-	n-Decane	142	2.2	174	0.73	23.83	44.24		46					0
Pure n- iso-	n-dodecane	170	2.167	216	0.75	25.35	44.15		80	0.07701	73			0
Pure n- iso-	n-Heptane	100	2.286	98	0.683	20.14	44.57		-7	0.08021	53.5			0
Pure n- iso-	n-Hexane	86	2.333	69	0.664	18.43	44.75				49			0
Pure n- iso-	n-Nonane	128	2.222	151	0.719	22.85	44.31		31		60.9			0
Pure n- iso-	n-Pentadecane	212	2.133	270	0.769						96			0
Pure n- iso-	n-Tridecane	184	2.154	234	0.756						90			0
Pure n- iso-	n-Undecane	156	2.182	196	0.74	24.66	44.19		61		83			0
Pure n- iso-	Octane	114	2.25	126	0.702	21.61	44.43		12		58.2			0

Technical Report Documentation Page

1. Report No.	2. Government Accession No.	3. Recipient's Catalog No.
j.fuel.2019.115715		

4. Title and Subtitle	5. Report Date
On estimating physical and chemical properties of hydrocarbon fuels using mid-infrared FTIR spectra and regularized linear models	July 2019
	6. Performing Organization Code

7. Author(s)	8. Performing Organization Report No.
Yu Wang, Yiming Ding, Wei Wei, Yi Cao David F. Davidson Ronald K. Hanson	

9. Performing Organization Name and Address	10. Work Unit No. (TRAIS)
Center of Excellence for: Alternative Jet Fuels and Environment Stanford University Stanford CA 94305	11. Contract or Grant No. 13-C-AFJE-SU-15

12. Sponsoring Agency Name and Address	13. Type of Report and Period Covered
Federal Aviation Administration Office of Environment and Energy	14. Sponsoring Agency Code

15. Supplementary Notes

16. Abstract

The concept of a compact, economical FTIR-based analyzer for estimating the properties of hydrocarbon fuels with small amounts of fuel is proposed. The high correlations between mid-IR FTIR absorption spectra of fuel vapor in the range 3300–3550 nm and 15 physical and chemical properties, such as density, initial boiling point, surface tension, kinematic viscosity, number of carbon and hydrogen per average molecule, and derived cetane number, for 64 hydrocarbon fuels are demonstrated. Lasso-regularized linear models based on linear combination of absorption cross sections at selected wavelengths are built for each of these physical and chemical properties, yielding accurate estimations.

17. Key Words	18. Distribution Statement
Hydrocarbon fuel, Alternative fuel, Physical and chemical property, Combustion, Mid-IR spectroscopy, Generalized linear model, Machine learning, ASCENT	

19. Security Classif. (of this report)	20. Security Classif. (of this page)	21. No. of Pages	22. Price
Unclassified	Unclassified		